Bone Susceptibility Quantification: In Vivo Feasibility with MR Source QUantification by Inverting the Dipole field

L. de Rochefort[1], R. Brown[1], M. R. Prince[1], and Y. Wang[1]
[1]Radiology, Weill Medical College of Cornell University, New York, NY, United States

PURPOSE

Bone mineral density (BMD) is an important parameter for evaluating osteoporosis and other bone diseases. To avoid invasive biopsy and exposure to ionizing radiation, there have been several works using MRI to quantify bone density (1, 2). One approach makes use of the susceptibility difference between the various constituents of bone tissue, which is linked to its composition (3). Bone volume susceptibility has been measured in vitro by fitting observed field shifts of trabecular bone MR micro images (4) or by utilizing T2* effects of solid bone powder diluted in liquids (5). Here we show the in vivo feasibility of MR-SQUID (Magnetic Resonance Source QUantification by Inverting the Dipole field). Magnetic susceptibility of solid bones is measured by fitting the observed field shifts (from the signal phase) to a field model built from segmented signal intensity images.

MATERIAL AND METHODS

Experiments were performed at 3T. An interleaved multi-echo 2D spoiled gradient-echo sequence was used with FOV=13 cm, 128^2 matrix, slice-thickness=5 mm, BW=62.5 kHz with full-echo readouts, TR=8.7, TE=2.1, 3.1, 4.1, 5.1, 6.1 ms, FA=30°, and a quadrature birdcage coil used for foot imaging. For the in vitro experiment, a reference acquisition was performed on a 15-cm long, 8-cm diameter cylinder placed perpendicular to B0. Then, an identical acquisition was performed after placement of a 10-cm long lamb-leg bone inside the cylinder. In vivo, acquisition was performed on a 26 yo male volunteer's forearm placed perpendicular to B0.
To extract the field shifts, a weighted linear least-square algorithm was applied to each voxel to fit the phase temporal evolution with an affine model. A 3D soft segmentation algorithm was implemented to define regions of constant susceptibility from magnitude images and converted to a 3D surface mesh. In vitro, the following regions were defined: 1) solid bone and 2) marrow; in vivo, 1) the arm, 2) ulna, 3) ulna marrow, 4) radius, 5) radius marrow.
Making use of magnetostatic Maxwell equation linearity (6), the contribution to the observed field shift of a region of constant susceptibility χ, given its shape and its orientation with respect to B0, is given at any point p by: χD_p, i.e. the product of susceptibility and the shape factor (convolution of the shape by a dipole field) that can be calculated from the boundary element method (7). Taking into account marrow's chemical shift, the following linear systems were solved using standard linear least-square excluding the field measured inside the bone (which had no proton signal):
In vitro: the field difference between bone and reference acquisitions at any point p was modeled by $\delta_p=\Delta\chi_{bone\text{-}water}D_{bone,p}+\Delta\chi_{marrow\text{-}water}D_{marrow,p}+\Delta\sigma_{marrow\text{-}water}I_{marrow,p}$, where $\Delta\chi$ refers to susceptibility, $\Delta\sigma$ to chemical shift and I_{marrow} indicates whether or not the point p is inside the marrow.
In vivo: the field was similarly modeled considering arm, bone and marrow susceptibilities and marrow chemical shifts. A linear order shimming correction was also added to account for frequency centering and long range effects of unmodeled objects: $+\delta_0+g_xp_x+g_yp_y+g_zp_z$, where p_x, p_y and p_z refer to p coordinates. Different combinations where tested to stabilize the inversion process (Table 1).

RESULTS

Typical dipolar patterns were observed surrounding the bones (Fig.1, 2) and the field was much lower inside fatty marrow. No signal was obtained inside the solid bones, as expected, allowing a simple segmentation (Fig.3). After the inversion process, the fitted field matched fairly well the measured one (Fig.4). In vitro, bone susceptibility of -2.46 ppm relatively to water was obtained, value consistent with literature data (5) showing that bone is more diamagnetic than tissue. Marrow susceptibility (0.90 ppm) and chemical shift (-3.52 ppm) matched the values for fat. In vivo (Table 1), similar values and arm susceptibility close to water were obtained.

	Bone		Marrow				Arm
Combination	$\Delta\chi_{ulna\text{-}arm}$	$\Delta\chi_{radius\text{-}arm}$	$\Delta\chi_{ulna\text{-}arm}$	$\Delta\chi_{radius\text{-}arm}$	$\Delta\sigma_{ulna\text{-}arm}$	$\Delta\sigma_{radius\text{-}arm}$	χ_{arm}
Group	-2.18		0.85		-3.43		-8.94
CS set	-2.30	-1.83	0.60	0.50	**-3.50**		-8.98
No prior	-2.14	-1.82	-0.06	0.46	-3.61	-3.51	-9.00

Table 1: In vivo results for different combinations, by grouping the bone, imposing chemical shift value for the marrow (bold number), or keeping every unknown (no prior).

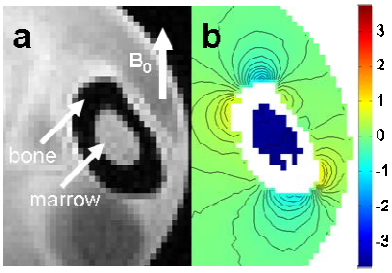

Fig. 1: In vitro coronal signal intensity map (a). Field in ppm together with contours (b).

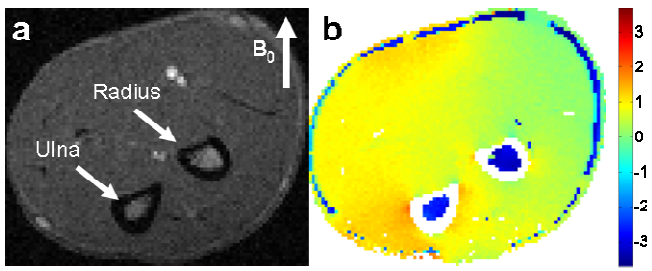

Fig. 2: In vivo coronal intensity map (a) and field map (b). Note the chemical shift for the marrow and subcutaneous fat.

DISCUSSION AND CONCLUSION

MR-SQUID was successfully applied in vitro and in vivo on long bones. Susceptibility values consistent with previous in vitro studies were obtained by measuring the field shifts from the signal phase and fitting them to a model extracted from the signal intensity images. On the forearm, improved results were found by implementing prior knowledge such as the fatty marrow chemical shift or by reducing the number of variables by grouping regions such as the radius and ulna. Additionally, linear shimming offered suitable correction for errors introduced by non-modeled objects far from the forearm.
MR-SQUID is a fast, non-invasive tool to quantify susceptibilities in vivo that could be applied to characterize bone and marrow diseases.

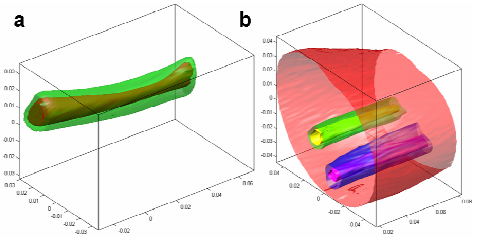

Fig. 3: 3D rendering of the segmented regions for the in vitro (a) and the in vivo (b) experiments.

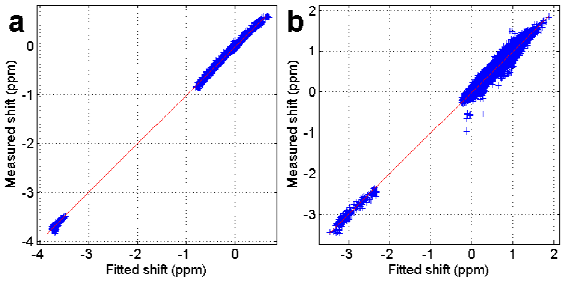

Fig. 4: Measured field vs fitted field in vitro (a) and in vivo (b).

REFERENCES

1. Schick et al., Invest Radiol 1995, 30p254 **2.** Wehrli et al., JMRI 2004, 20p83 **3**. Elliott et al., J Bone Joint Surg Am 1957, 39p167 **4.** Chung et al., JMR B 1996, 113p-172 **5.** Hopkins et al., MRM 1997, 37p494 **6.** Jackson, Classical electrodynamics, 3rd edition: Wiley and Sons; 1999 **7.** de Munck et al., IEEE TMI 1996, 15p620